Stokes flows in deformable conduits: Hydrodynamic resistance beyond Poiseuille

Ivan C. Christov[†] and TMNT-Lab[‡] members Vishal Anand, Tanmay C. Shidhore, and Xiaojia Wang

School of Mechanical Engineering, Purdue University, West Lafayette, Indiana, USA; [†]christov@pudue.edu, [‡] tmnt-lab.org

Introduction

Preliminaries:

- Consider a long and shallow microchannel (blue area in Fig. 1) such that $h_0 \ll w \ll l$.
- The microchannel is embedded in a soft material (e.g., PDMS); the bottom is rigid.
- Only top wall deformation is considered because $h_0 \ll w \Rightarrow$ the deformation of side walls is negligible.

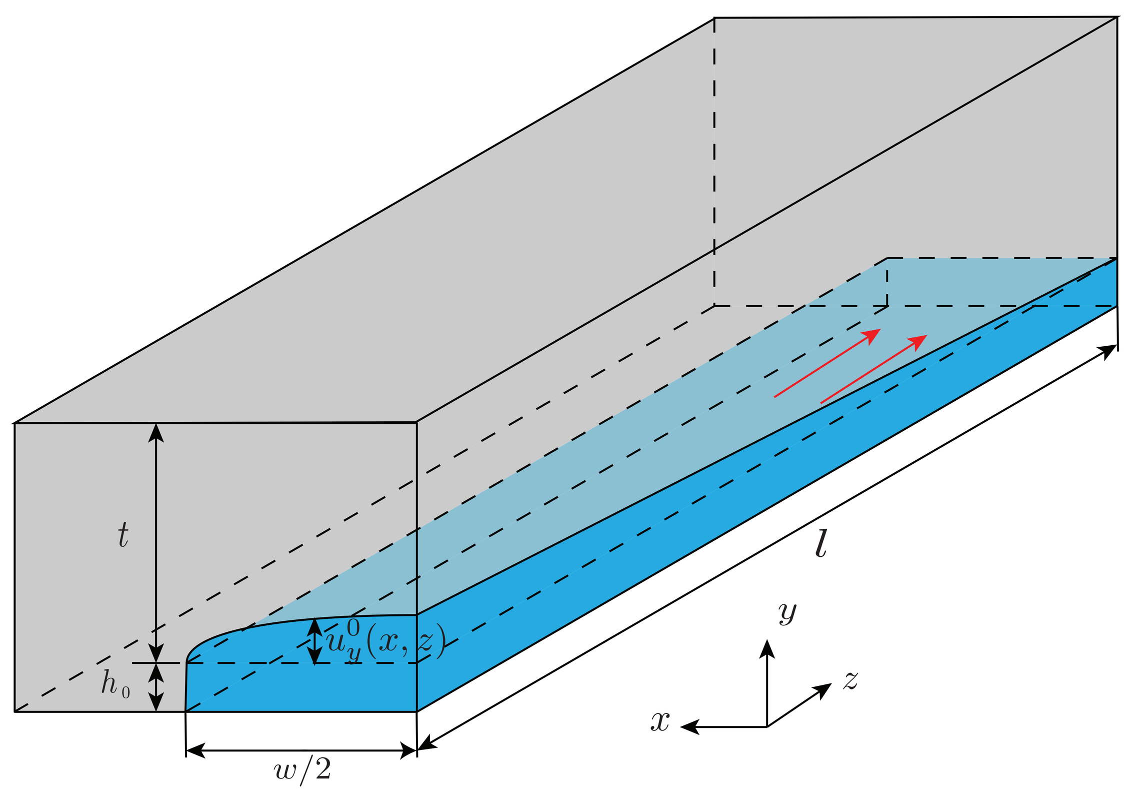

Figure 1: Schematic diagram of a compliant microchannel embedded in PDMS. The origin of the coordinate system is the undeformed fluid–solid interface, initially h_0 above the rigid bottom.

Lubrication approximation for flow in shallow channels

- For a long and shallow microchannel, to the leading order in the perturbation parameters $\epsilon := h_0/l$ and $\delta := h_0/w$ ($\epsilon \ll \delta \ll 1$), the incompressible Navier–Stokes equations reduce to

$$\frac{\partial v_x}{\partial x} + \frac{\partial v_y}{\partial y} + \frac{\partial v_z}{\partial z} = 0, \qquad 0 = -\frac{\partial p}{\partial x} = \frac{\partial p}{\partial y}, \qquad 0 = -\frac{\partial p}{\partial z} + \mu \frac{\partial^2 v_z}{\partial y^2}.$$

- The leading order solution (the lubrication approximation) is axial flow ($v_y \simeq v_x \simeq 0$):

$$v_z(x,y,z) = \frac{1}{2\mu}\frac{dp}{dz}(y + h_0)\left[y - u_y^0(x,z)\right] \qquad \left(-h_0 \le y \le u_y^0\right). \tag{1}$$

But, $dp/dz \neq const.$ due to the axially varying deformation $u_y^0(x,z)$ of the fluid–solid interface.

Shape of the fluid–solid interface: Thin structures

- Assumptions:
  1. The deformation is small enough so that we can use isotropic linear elasticity.
  2. Since $w, t \ll l$, the deformation of each flow-wise cross-section is decoupled as $\epsilon \to 0$ [CCSS18].
  3. The wall's maximum displacement is small, and the structure is thin: $u_{max} \ll t \sim h_0 \ll w$.
- Using first-order shear-deformation plate theory with clamped BCs [SC18], the displacement is

$$u_y^0(x,z) = \frac{w\,p(z)}{\overline{E}_Y} \underbrace{\left(\frac{w}{t}\right)^3 \frac{1}{2}\left[\frac{1}{4} - \left(\frac{x}{w}\right)^2\right]\left\{\frac{2(t/w)^2}{(1-\nu)} + \left[\frac{1}{4} - \left(\frac{x}{w}\right)^2\right]\right\}}_{\mathfrak{G}_{\mathrm{plate}}(x/w,t/w)}, \tag{2}$$

where $\overline{E}_Y = E_Y/(1-\nu^2)$ is a scaled Young's modulus E_Y, and ν is the Poisson ratio.

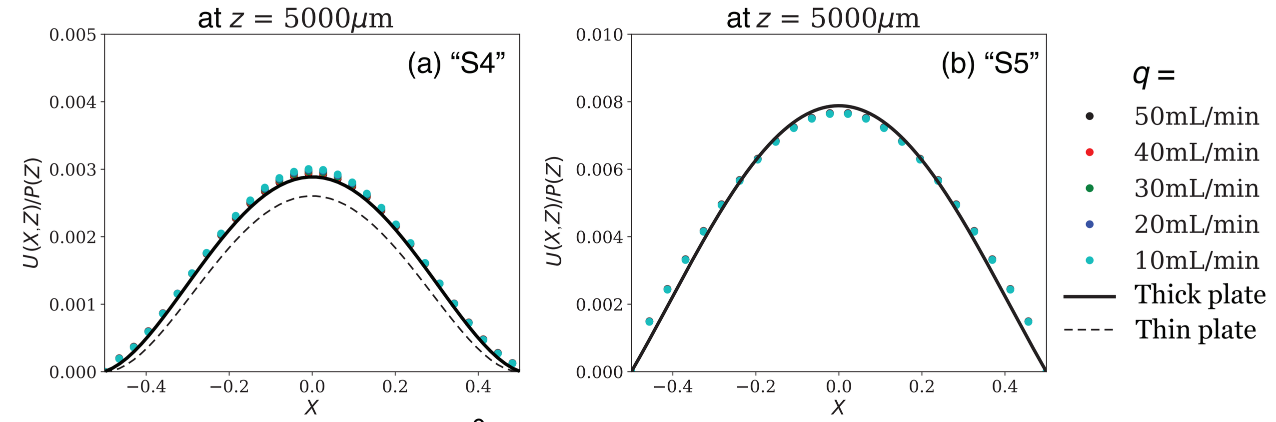

Figure 2: Dimensionless ratio of u_y^0 and p from (2) showing collapse across flow rates. Symbols from ANSYS fluid–structure interaction simulations [SC18] matched to experiments from [OYE13]. Thin-plate theory corresponds to $t/w \to 0$ in $\{\cdot\}$ in (2). (a) $t/w \simeq 0.12$, (b) $t/w \simeq 0.35$.

Shape of the fluid–solid interface: Thick structures

- Assumptions:
  1. The deformation is small enough so that we can use isotropic linear elasticity.
  2. Since $w \ll l$ and $t \ll l$, the top wall is in a plane strain configuration.
  3. At the side walls, $\sigma_{xx} \sim p h_0/t$ and $t \sim w \gg h_0$ (thick structure) $\Rightarrow$ use a simply supported boundary condition in each cross-section: $\sigma_{xx}|_{x=\pm w/2} = 0$.
- Using an Airy stress function for a simply supported rectangle, subject to the BCs $\sigma_{yy}|_{y=0} = -p(z)$ and $\sigma_{xy}|_{y=0} = \sigma_{yy}|_{y=t} = \sigma_{xy}|_{y=t} = 0$, we obtain the displacement as a Fourier series [WC19]:

$$u_y^0(x,z) = \frac{w\,p(z)}{\overline{E}_Y} \underbrace{\sum_{m=1}^{\infty} \frac{4}{m^2\pi^2}[1-(-1)^m] \sin\left[m\pi\left(\frac{x}{w} + \frac{1}{2}\right)\right]}_{\mathfrak{G}_{\mathrm{halfspace}}(x/w)} \qquad (t^2/w^2 \to \infty). \tag{3}$$

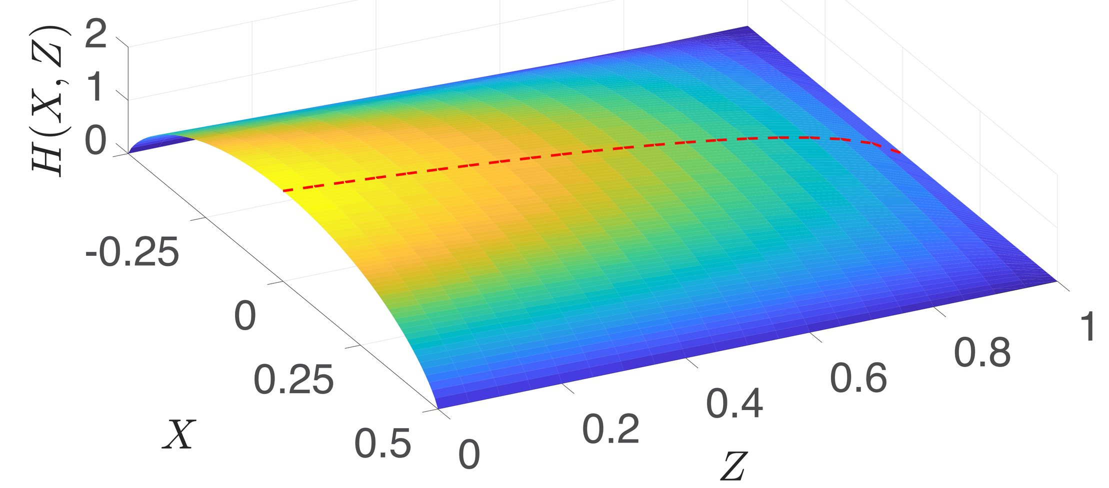

Figure 3: Dimensionless deformed fluid–solid interface, $H(X,Z) = u_y^0(x/w, z/l)/h_0$, from equation (3) with $p(z)$ having been obtained from (4); from [WC19].

The flow rate–pressure drop relation

- The volumetric flow rate across the deformed cross-section is defined as

$$q = \int_{-w/2}^{+w/2}\int_{-h_0}^{u_y^0(x,z)} v_z(x,y,z)\,dy\,dx \overset{\text{using (1)}}{=} -\frac{1}{12\mu}\frac{dp}{dz}\int_{-w/2}^{+w/2}\left[h_0 + u_y^0(x,z)\right]^3 dx.$$

- In steady flow with $q = const.$ controlled, set outlet to gauge $p(l) = 0$, use $u_y^0(x,z)$ derived to obtain

$$q = \frac{h_0^3 w\,p(z)}{12\mu(l-z)}\left[1 + \left(\frac{w}{\overline{E}_Y h_0}\right) S_1\, p(z) + \left(\frac{w}{\overline{E}_Y h_0}\right)^2 S_2\, p(z)^2 + \left(\frac{w}{\overline{E}_Y h_0}\right)^3 S_3\, p(z)^3\right], \tag{4}$$

where $S_1 = \frac{3}{2}\int_{-1/2}^{+1/2}\mathfrak{G}\,dX$, $S_2 = \int_{-1/2}^{+1/2}\mathfrak{G}^2\,dX$, $S_3 = \frac{1}{4}\int_{-1/2}^{+1/2}\mathfrak{G}^3\,dX$ are evaluated from (2) or (3).

- Flow rate–pressure drop relation (4) (no free parameters) agrees well with experiments & simulations.

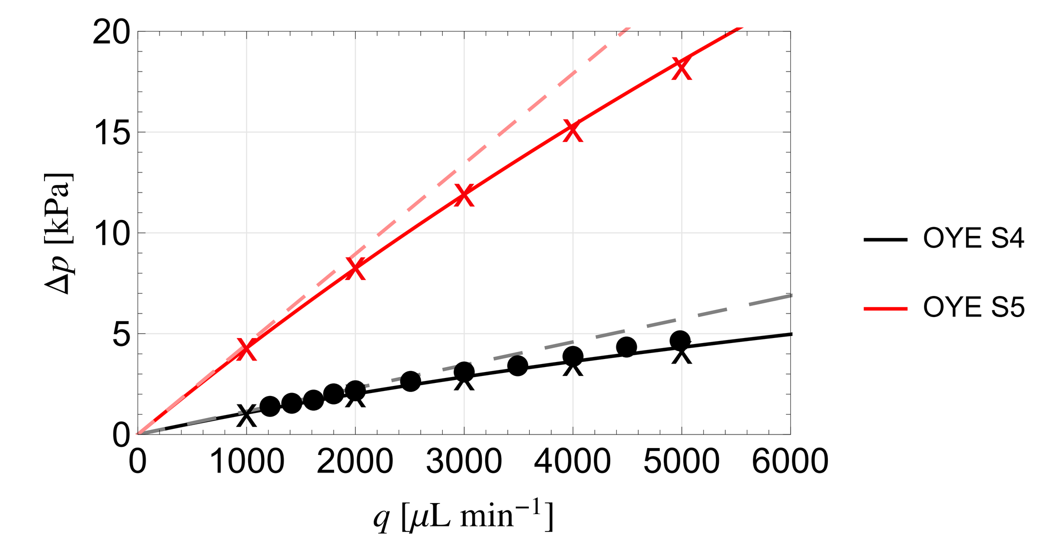

Figure 4: Comparison between the **thin**-structure theory (4) with (2) (solid), Poiseuille's law (dashed), and two sets of simulations ($\times$) [SC18] tuned to experiments ($\bullet$) [OYE13].

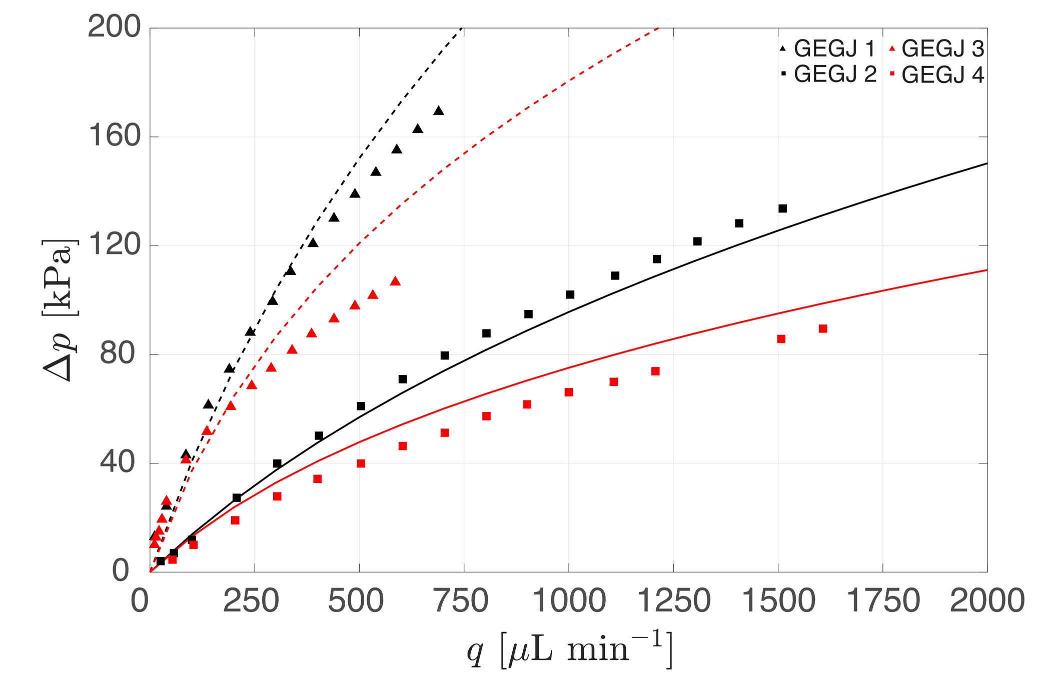

Figure 5: Comparison between the **thick**-structure theory (4) with (3) (curves) and four experiments (symbols) from [GEGJ06].

- We have also studied non-Newtonian fluids [ADJC19]; ideas carry over but can't solve ODE for $p(z)$.

In summary: We constructed predictive models of pressure drops in compliant rectangular conduits under different deformation regimes. In doing so, we rationalized previous experiments.
$\Rightarrow$ Nonlinear (flow-responsive) resistive elements within the hydraulic circuit analogy!
Rigorously generalized Poiseuille's law, i.e., $\Delta p = \frac{12\mu l q}{h_0^3 w}\left[1 + \mathcal{F}(\Delta p/E, w/h_0, t/w, \ldots)\right]$.

Acknowledgements: This research is supported, in part, by funding from the U.S. National Science Foundation (NSF) under Grant CBET-1705637.

References

[ADJC19] V. Anand, J. David JR, and I. C. Christov. Non-Newtonian fluid–structure interactions: Static response of a microchannel due to internal flow of a power-law fluid. *J. Non-Newtonian Fluid Mech.*, 264:62–72, 2019.

[CCSS18] I. C. Christov, V. Cognet, T. C. Shidhore, and H. A. Stone. Flow rate–pressure drop relation for deformable shallow microfluidic channels. *J. Fluid Mech.*, 814:267–286, 2018.

[GEGJ06] T. Gervais, J. El-Ali, A. Günther, and K. F. Jensen. Flow-induced deformation of shallow microfluidic channels. *Lab Chip*, 6:500–507, 2006.

[OYE13] O. Ozsun, V. Yakhot, and K. L. Ekinci. Non-invasive measurement of the pressure distribution in a deformable micro-channel. *J. Fluid Mech.*, 734:R1, 2013.

[SC18] T. C. Shidhore and I. C. Christov. Static response of deformable microchannels: a comparative modelling study. *J. Phys.: Condens. Matter*, 30:054002, 2018.

[WC19] X. Wang and I. C. Christov. Theory of the flow-induced deformation of shallow compliant microchannels with thick walls. *preprint*, arXiv:1908.03556, 2019.